© 2019. Published by The Company of Biologists Ltd | Journal of Experimental Biology (2019) 222, jeb188508. doi:10.1242/jeb.188508

RESEARCH ARTICLE

Parasitic gut infection in *Libellula pulchella* causes functional and molecular resemblance of dragonfly flight muscle to skeletal muscle of obese vertebrates

Rudolf J. Schilder[1,2,*] and Hannah Stewart[1]

ABSTRACT

We previously demonstrated the existence of a naturally occurring metabolic disease phenotype in *Libellula pulchella* dragonflies that shows high similarity to vertebrate obesity and type II diabetes, and is caused by a protozoan gut parasite. To further mechanistic understanding of how this metabolic disease phenotype affects fitness of male *L. pulchella in vivo*, we examined infection effects on *in situ* muscle performance and molecular traits relevant to dragonfly flight performance in nature. Importantly, these traits were previously shown to be affected in obese vertebrates. Similarly to obesity effects in rat skeletal muscle, dragonfly gut infection caused a disruption of relationships between body mass, flight muscle power output and alternative pre-mRNA splicing of troponin T, which affects muscle calcium sensitivity and performance in insects and vertebrates. In addition, when simulated *in situ* to contract at cycle frequencies ranging from 20 to 45 Hz, flight muscles of infected individuals displayed a left shift in power–cycle frequency curves, indicating a significant reduction in their optimal cycle frequency. Interestingly, these power–cycle curves were similar to those produced by flight muscles of non-infected teneral (i.e. physiologically immature) adult *L. pulchella* males. Overall, our results indicate that the effects of metabolic disease on skeletal muscle physiology in natural insect systems are similar to those observed in vertebrates maintained in laboratory settings. More generally, they indicate that study of natural, host–parasite interactions can contribute important insight into how environmental factors other than diet and exercise may contribute to the development of metabolic disease phenotypes.

KEY WORDS: Infection, Obesity, Muscle performance, Dragonfly, Troponin T, Contraction frequency

INTRODUCTION

Obesity is a common metabolic disease in humans and can be induced in laboratory animals by feeding with a high-fat diet (Birse et al., 2010; Fenton and Dowling, 1953; Ingle, 1949). Interestingly, a recent meta-analysis demonstrated that during the past five decades, obesity has also become common in laboratory mammals, and feral (rural and urban) rodents and domestic pets that are not exposed to high-fat diets and lack of exercise (Klimentidis et al., 2011). This suggests that, in addition to genetic predisposition, there are other factors that can contribute to the development of metabolic disease. Infections by viral, bacterial and protozoan agents are considered such factors, and may affect host metabolic health in various ways, including endocrine modulation, enhanced expression of genes controlling adipogenic and lipogenic pathways (Dhurandhar, 2011; McAllister et al., 2009; Pasarica and Dhurandhar, 2007), or possibly, through changes to the composition of the gut microbiome and/or induction of a systemic inflammatory state (Sonnenburg et al., 2006; Steinberg, 2007; Turnbaugh et al., 2006). This potential for infectious origins of metabolic disease is interesting because it opens a path to examine their mechanistic bases in non-model, vertebrate and insect hosts faced with infection risks in nature. Given the evolutionarily conserved nature of cellular pathways controlling energy storage, catabolism, and aspects of immunity in vertebrates and insects (Sacktor 1975; Schlegel and Stainier, 2007; Arrese and Soulages, 2010; Kimbrell and Beutler, 2001; Hoffmann et al., 1999; Palmer and Jiggins, 2015; Martinelli and Reichhart, 2005; Beutler, 2004), there are likely interesting parallels between the physiological underpinnings of infection-associated metabolic impairments in these systems.

Insect species whose fitness crucially depends on flight make for potentially useful subjects to study such parallels. Because of the high energetic cost of this locomotor mode (e.g. Sacktor 1975 in Candy and Kilby, 1975; Gilmour 1965), flight motor designs that are optimized for high mechanical performance and energy catabolism, will need equally fine-tuned, homeostatic interactions with digestive, energy anabolic and nutrient mobilization physiology. In a fashion similar to how a high-performance race car differs from a mini-van (Marden et al., 1999; Mead et al., 2017), flying insects may have lower built-in safety factors that protect against disturbances of these homeostatic interactions than non-flying insects, and show more pronounced effects of infections. Studies of the effects of parasitic infections on insect flight performance traits have focused mainly on mosquitos and honeybees (e.g. Rowland and Boersma, 1988; Yee and Anderson, 1995; Wolf et al., 2014; Dosselli et al., 2016; Newman, Anderson, and Goldberg, 2016; Dussaubat et al., 2013; but see Altizer et al., 2015), but mechanistic details of infection effects are rarely studied (but see Harrison et al., 2001).

We previously reported that infection of *Libellula pulchella* dragonflies with protozoan intestinal parasites (Apicomplexa: Eugregarinorida, *Hoplorrhynchus* sp., also known as 'gregarines') causes a metabolic disease syndrome involving a doubling of hemolymph total carbohydrate concentration, a significant increase (26%) in mean thoracic lipid content, chronic stress/inflammation pathway activation and a reduced ability to oxidize fatty acids by flight muscles (Schilder and Marden, 2006). These symptoms are very similar to mammalian metabolic disease phenotypes such as obesity and type II diabetes (Goodpaster and Wolf, 2004; Kelley and Goodpaster, 2001; Khovidhunkit et al., 2004; Perseghin, 2005;

[1]Pennsylvania State University, Department of Entomology, 501 Ag Sciences & Industries Building, State College, PA 16802, USA. [2]Pennsylvania State University, Department of Biology, 501 Ag Sciences & Industries Building, State College, PA 16802, USA.

*Author for correspondence (rjs360@psu.edu)

R.J.S., 0000-0003-1229-1274

Received 9 July 2018; Accepted 11 January 2019

Journal of Experimental Biology (2019) 222, jeb188508. doi:10.1242/jeb.188508

Ritov et al., 2005). In addition to these metabolic impairments, we demonstrated that gregarine infection causes reduced mass-specific flight muscle performance in *L. pulchella* dragonflies (Schilder and Marden, 2006), which is similar to the decline in skeletal muscle performance generally observed in vertebrate obesity (Bollinger, 2017; Lafortuna et al., 2005; Maffiuletti et al., 2007; Seebacher et al., 2017; Tallis et al., 2017; Tallis et al., 2018; Tomlinson et al., 2016).

The mechanism(s) underlying reduction of mass-specific muscle performance during metabolic disease are poorly understood, but likely affect muscle sarcomere function at a molecular level. In vertebrates, a role for obesity-associated shifts in the composition of muscle fiber types, as a result of changes in expression of myosin heavy chain genes (*Myhc*), has been indicated. However, no single satisfactory explanatory principle has been uncovered, as the effects of obesity on muscle fiber type can vary from slow-to-fast shifts (i.e. MyHC type I→MyHC type II) to fast-to-slow shifts, or can be absent altogether, depending on the species and muscle examined (DeNies et al., 2014; Schönke et al., 2018; Tallis et al., 2017; Tanner et al., 2002).

Whether MyHC isoform composition has any role in infection-associated decline of muscle function in *L. pulchella* is unclear. Insect flight muscle is generally not believed to express multiple fiber types that differ in MyHC isoform composition (Ayme-Southgate et al., 2015; Hooper and Thuma, 2005) and contractile properties. However, two recent studies suggest that multiple *Myhc* mRNAs can be expressed in *Manduca sexta* and *Locusta migratoria* flight muscle tissue (Ayme-Southgate et al., 2015; Li et al., 2016). Although it is not known whether these mRNAs are translated into functional MyHC protein isoforms for *M. sexta*, Ziegler et al. (1994) reported the presence of two distinct MyHC protein isoforms in flight muscle of *L. migratoria* (and the fly *Phormia terraenovae*). However, if and how these different MyHC protein isoforms affect flight muscle function is unknown. Effects of transgenic insertion of different *Myhc* genes on muscle contractile properties have been detailed in *Drosophila* (reviewed in Maughan and Swank, 2013), but naturally occurring shifts in MyHC protein isoforms with functional consequences have, to our knowledge, not been reported for adult insect flight muscle.

In contrast, isoform expression of another key regulatory sarcomere protein, troponin T (Tnt), varies significantly in flight muscles of male *L. pulchella* obtained from wild populations and does affect flight muscle function (Fitzhugh and Marden, 1997; Marden et al., 1999; Marden et al., 2001). Similarly to insect *Myhc*, variation in *Tnt* isoform expression is generated by alternative pre-mRNA splicing. Importantly, the relative abundance of one of two highly abundant *Tnt* mRNA splice variants (i.e. *Lp_Tnt261*; see Table 1) in *L. pulchella* flight muscle was shown to correlate positively with maximum mass-specific flight muscle force and power output, wingbeat frequency use in free flight, and muscle fiber calcium sensitivity (Marden et al., 2001). These findings are consistent with a rich vertebrate literature describing effects of variation in Tnt protein isoforms on muscle calcium sensitivity (Greaser et al., 1988; Nassar et al., 1991; Reiser et al., 1990; Schachat et al., 1987), and the general idea that varying muscle calcium sensitivity affects acto-myosin cross-bridge recruitment, and thus the rate and amount of force development, and power output (Marden et al., 2001; Moss et al., 1995; Perry, 1998; Solaro and Rarick, 1998; Sweeney et al., 1993).

In rat load-bearing muscle (i.e. gastrocnemius), we recently demonstrated that obesity causes a mismatch between body mass and *Tnt* alternative pre-mRNA splicing (Black et al., 2017; Schilder et al., 2011). Thus, rat skeletal muscle *Tnt* expression of >300 g obese rats resembles that of much younger (<150 g), non-obese specimens. In contrast, experiments in non-obese, healthy rats, flies (*Drosophila melanogaster*) and moths (*Spodoptera frugiperda*), demonstrated that the relative abundance of *Tnt* mRNAs splice variants in load-bearing muscle is adjusted in proportion to body weight increase resulting from natural growth or experimental body weight manipulations (Marden et al., 2008; Schilder and Raynor, 2017; Schilder et al., 2011). Obesity therefore appears to cause an impairment of a sensing mechanism that relates body weight to skeletal muscle molecular composition. Importantly, the *Tnt* expression pattern in obese rats is expected to lower muscle calcium sensitivity and force output (Briggs and Schachat, 1996; Schachat et al., 1987; Schilder et al., 2011). This, in turn, is predicted to reduce muscle mass-specific performance, as demonstrated in aging humans (Coble et al., 2015) and, as mentioned earlier, in obese mammals (Tallis et al., 2017) and gregarine-infected dragonflies (Schilder and Marden, 2006). However, it is currently unknown if the metabolic syndrome associated with gregarine infection of *L. pulchella* affects relationships between *Tnt* expression, body mass and flight muscle performance in an similar fashion to that observed in rats.

More potential overlap between the obesity phenotypes in vertebrates and dragonflies was indicated by a recent study on zebrafish (Seebacher et al., 2017), which showed that mass-specific power output by locomotor muscle of obese zebrafish declined specifically at higher contraction frequencies. Territorial behavior of non-infected *L. pulchella* males involves the use of high-frequency wing beats (Dudley, 2002; May, 1991; Rüppell, 1989), powered by equally high flight muscle contraction frequencies. In contrast, gregarine-infected male *L. pulchella* are relatively inactive and avoid territorial disputes (Marden and Cobb, 2004). Interestingly, this behavior resembles that of recently eclosed, physiologically immature 'teneral' male *L. pulchella*, which do not engage in territorial disputes, but instead focus on foraging. Pertinent to the current study, teneral *L. pulchella* employ significantly lower wing beat frequencies, and display significantly lower flight muscle fiber

Table 1. Expression of *Tnt* splice variants in *L. pulchella* flight muscle

		Infection status		
Splice variant	Relative abundance	NI	II	MI
Tnt_Lp243	0.04±0.007 (0–0.17)	0.03±0.006	0.05±0.01	0.06±0.02
Tnt_Lp246	0.06±0.007 (0–0.21)	0.05±0.006	0.06±0.01	0.09±0.03
Tnt_Lp258	0.59±0.01 (0.37–0.76)	0.60±0.02	0.58±0.05	0.58±0.04
Tnt_Lp261	0.26±0.01 (0.14–0.38)	0.28±0.01	0.23±0.02	0.21±0.03
Tnt_Lp267	0.04±0.006 (0–0.17)	0.04±0.007	0.06±0.007	0.04±0.02
Tnt_Lp270	0.01±0.002 (0–0.06)	0.009±0.002	0.02±0.009	0.008±0.002

Overall and infection status-specific mean relative abundance (±s.e.m.; *N*=38; 24 NI, 6 II, 8 MI) and relative abundance range (in parentheses) for six *Tnt* splice variants. Splice variant designation reflects unique amplicon lengths.

calcium sensitivity compared with mature males (Marden et al., 1998). Thus, gregarine infection may prevent *L. pulchella* males from participating in territorial behavior by affecting their ability to operate competitively at higher contractile frequencies.

Combined, these observations and findings suggest there are similarities at the level of behavior, muscle contractile performance and molecular composition between locomotor muscles of obese vertebrates and infected *L. pulchella* males, and also between infected mature and non-infected teneral *L. pulchella* males. Here, we first tested the hypothesis that gregarine infection causes a mismatch between body mass, flight muscle *Tnt* alternative splicing pattern and maximum flight muscle performance in this species. In addition, in a similar fashion to the Seebacher et al. (2017) zebrafish study, we tested the hypothesis that gregarine infection causes a left shift for the optimum of flight muscle power–cycle frequency curves (i.e. they are predicted to lose power output capacity at higher cycle frequencies), and compared these power–cycle frequency curves with those produced by teneral *L. pulchella* flight muscles.

MATERIALS AND METHODS

Animal samples

Mature adult male *Libellula pulchella* (Drury 1770) dragonflies were caught at several ponds located within a 7–8 mile radius around the Pennsylvania State University campus (University Park, PA, USA). Teneral (recently emerged, immature) adult males were caught at the periphery of these ponds, and identified by overall coloration (i.e. lack of abdominal purple pruinescence seen in mature males), flight behavior and the presence of a rainbow-colored sheen on their wings. After capture, dragonflies were transported to the laboratory in cooled plastic containers containing a moistened paper towel. All animals were used in experiments within 2–6 h of capture. After experiments and determination of infection status and body composition values (see below), basalar muscles (muscle dvm3; Simmons, 1977) were placed in a cryo-vial and flash frozen in a liquid nitrogen Dewar, after which the tubes were stored under liquid nitrogen or at −80°C until used. The remaining carcasses were similarly stored, but separate from the basalar muscles.

Infection status and body composition

It is important to note that we were blind to an individual's gregarine (*Hoplorrhynchus* sp.) infection status until the end of experiments, when parasite load was assessed by surgically opening the midgut *post mortem*. Our previous work in this system demonstrated that flight muscle performance of male dragonflies is affected significantly only when a mature infection is present compared with when an immature infection is present (Schilder and Marden, 2006). As in that study, an infection was therefore classified as immature if small gregarine trophozoites were observed, but no fully grown (sexually mature) gregarine trophozoites (the feeding stage of gregarines; Smith and Clopton, 2003) were present. An infection was classified as mature if one or more fully grown gregarine trophozoites were present, regardless of whether any additional smaller trophozoites were present. Body mass, thoracic mass, abdominal mass, and flight (basalar) muscle mass were measured to the nearest 0.1 mg by means of a Mettler AE100 scale.

Flight muscle performance assays

In situ flight muscle performance was determined using the work loop technique described previously, applied to the basalar muscle (Marden et al., 2001; Schilder and Marden, 2004). Briefly, dragonflies (N=65 mature, N=11 teneral) were decapitated and wings and legs were clipped off, after which the basalar muscle was mechanically isolated from the rest of the thorax via several small incisions around the humoral plate. A fine suture was then tied around the apodeme and glued to a modified insect pin suspended from the lever arm of a lever system (Cambridge Technology 300B, Cambridge, MA, USA). Imposed strain was set to 0.52 mm, which is 10% of mean basalar muscle length for this species. The preparation was electrically stimulated with 0.25 ms, 0.5 V pulses, initiated at 44% of lengthening phase (Marden et al., 2001). Net work produced by the basalar muscle during strain cycles was calculated using the work loop area produced during the fourth of a total of five length cycles imposed at frequencies varying between 20 and 45 Hz. Muscle power output at a given cycle frequency was calculated as net muscle work divided by period (i.e. frequency^{-1}), and standardized by dividing by muscle mass (i.e. mass-specific power output; W kg^{-1} muscle). Thoracic temperature was monitored using a fine-gauge thermocouple that was inserted into the metathorax and connected to a TC-1000 thermometer (Sable Systems, Las Vegas, NV, USA). Thoracic temperature during these assays was regulated between 32 and 34°C using a water circulator that pumped water through an aluminium stage to which the preparation was affixed. Data acquisition and hardware timing was controlled through custom scripts in Igor Pro v6.3 software, via a National Instruments Multifunction I/O board (NI-6011E). For an independent set of dragonflies (N=38), we used the same protocol but determined maximum mass-specific power output at any contractile frequency, which was subsequently correlated with body mass, and relative abundance of *Lp_Tnt261* and *Lp_Tnt258*, the two most abundant *Tnt* mRNA splice variants (Table 1).

Quantification of *Tnt* splice variant relative abundance

Tnt splice variant expression was analyzed in similar fashion to previous insect studies on this gene (Marden et al., 1999; Schilder and Raynor, 2017). Briefly, total RNA was extracted from frozen basalar muscle using Trizol reagent (Invitrogen, Carlsbad, CA, USA), precipitated in isopropanol and washed in ethanol, according to the manufacturer's instructions. Total poly-A mRNA was reverse transcribed using a Superscript III reverse transcriptase kit (Invitrogen) and a custom primer (ATTCTAGAGGCCGAGGCG-GCCGACATGdT$_{30}$-VN). *L. pulchella* flight muscle *Tnt* splice variants, previously identified by Marden et al., 1999, were amplified from cDNA samples using a fluorescein (FAM)-labeled forward primer 5′-6FAM-CGCTTCTTTCACTCGTTGTTCAAAC-3′ and reverse primer 5′-CCTTCGCTTGGCTTGCTTC-3′. 6FAM-labeled PCR products obtained in this fashion were diluted 1:25 and separated by capillary electrophoresis (ABI DNA Analyzer, Applied Biosystems), after which the abundance of individual *Tnt* splice variants was quantified based on the amount of fluorescence detected. Relative abundance of individual *Tnt* splice variant amplicons was calculated by dividing out total *Tnt* splice variant fluorescence. *Tnt* splice variant amplicon size was calculated based on the GeneScan™ 500 LIZ™ dye internal size standard and GeneScan™ fragment analysis software (Applied Biosystems). *Tnt* splice variant amplicons were designated *Tnt_Lp2xx* based on amplicon size determined in this fashion (Table 1).

2D gel electrophoresis

The electrophoretic analyses of teneral basalar muscle samples (see Discussion) were performed as described previously (Schilder and Marden, 2007). Briefly, four muscle protein samples were prepared and separated using two-dimensional PAGE. Sample preparation was performed according to instructions provided with a MK-1

Journal of Experimental Biology (2019) 222, jeb188508. doi:10.1242/jeb.188508

tissue preparation kit (Kendrick Labs, Madison, WI, USA). Basalar muscles were first tested for contractile performance (see above) before being dissected out, homogenized in osmotic lysis buffer and heated in a SDS boiling buffer prior to being shipped to Kendrick Labs for 2D PAGE separation (see Schilder and Marden, 2007 for details). Gels were stained with Coomassie Brilliant Blue R-250 to allow protein identification and quantification. Protein spot profiles were analyzed from scanned 2D PAGE gel images using PD_Quest analysis software (Bio-Rad, Hercules, CA, USA). Quantities of the protein spot identified as a ∼155 kDa proteolytic degradation product of the full-length *Myhc* gene product were calculated as the percentage of total gel spot intensity and designated %MyHC155 (Schilder and Marden, 2007) and $\log_{10}$-transformed prior to statistical analyses. The location of five Tnt protein spots on scanned 2D PAGE gels were identified based on previous work that used a combination of gel electrophoresis and western blotting with an antibody against Tnt proteins (Marden et al., 1999). Quantities of individual Tnt protein spots were normalized to total quantities for all five Tnt protein spots. We then performed a principal component analysis of all Tnt protein spot data and used the first principal component (PC1 *Tnt* relative abundance) in our analyses that included previously published Tnt protein spot data for non-infected and infected mature adults (Schilder and Marden, 2007).

Statistics

We based our sampling on availability of field-collected specimens and previous experience with the *L. pulchella* system, instead of a formal *a priori* statistical power analysis. Statistical analyses were performed in JMP v12 (SAS Institute) or R v3.4.3 (R Foundation for Statistical Computing) software. Body and tissue mass comparisons were analyzed using one-way ANOVA, followed by either Student's *t*-tests or Tukey's HSD tests of group means where appropriate. *Tnt* splice variant relative abundances were arcsine transformed prior to statistical analyses, however, presented in figures and tables are actual, non-transformed relative abundances. Relationships between flight muscle power output, *Tnt* splice variant relative abundance and body mass were examined by linear regression and ANOVA. In addition, effects of infection on these relationships were examined using two-way ANOVA. The relationship between muscle power output and cycle frequency was analyzed with a mixed effect, two-way ANOVA using 'infection status', 'cycle frequency' and their interaction term as fixed effects, and 'frequency' nested within 'individual ID' as a random effect to account for the repeated-measures nature of this experiment (i.e. flight muscle from each individual underwent 25 length–stimulus cycles varying between 20 and 45 Hz). We used *post hoc* least-squares means contrast tests to identify significant differences between groups for power output at a given cycle frequency, with Bonferroni-adjusted critical α values. The 2D-PAGE protein expression data were analyzed via one-way ANOVA followed by Tukey's HSD tests of group means. A second-order polynomial fit was applied to the data presented. All reported ANOVA *F*-statistics are in the format $F_{x,xx}$, where $x=k-1$, and xx=number of observations−k, with k=number of groups. Effect sizes were calculated as η^2 or Cohen's d where appropriate (i.e. for model effects and *post hoc* pairwise mean comparisons, respectively). Graphs were generated in Igor Pro v8 (Wavemetrics, Inc; Portland, OR, USA).

RESULTS

Body composition

Gregarine infection had no effects on mature adult male *L. pulchella* body and tissue masses examined, as mean body, thorax, basalar muscle and abdomen mass, as well as the thorax:body mass ratio was not significantly different between non-infected (NI) *L. pulchella* and those with immature (II) or mature (MI) infections (Table 2).

However, when body mass variation was taken into account using a two-way ANOVA, infection was associated with a significantly higher basalar muscle mass ($F_{2,35}$=4.05; P=0.0264), and this effect was specific to MI individuals (*post hoc* Tukey HSD on least-square means: P=0.0283) as II individuals showed no significant differences from NI individuals (*post hoc* Tukey HSD on least-square means: P=0.961; Fig. 1A). Abdomen mass, thorax mass and the thorax:body mass ratio were not significantly different between groups when body mass variation was taken into account ($F_{2,35}$=0.015, P=0.985; $F_{2,35}$=1.270, P=0.293; $F_{2,35}$=1.265, P=0.295, respectively).

Tnt alternative splicing, muscle power output, and body mass

The relative abundance of *Tnt_Lp261*, the second most abundant *Tnt* splice variant in *L. pulchella* flight muscle (see Table 1) was positively correlated with maximum mass-specific power output ($F_{0,37}$=10.91, P=0.0022) among all individuals examined (Fig. 2A). A two-way ANOVA indicated that infection did not affect this relationship (i.e. the interaction term '*Tnt_Lp261**infection status' was not a significant contributor to the model; $F_{2,35}$=0.691, P=0.508), even though infection significantly reduced mean flight muscle power output ($F_{2,35}$=4.41, P=0.020). When infection status was taken into account in this fashion, relative abundance of *Tnt_Lp261* was no longer a significant predictor of maximum mass-specific power output ($F_{2,35}$=3.02, P=0.092).

There was no significant relationship between body mass and maximum flight muscle mass-specific power output ($F_{0,37}$=1.74, P=0.195) among all individuals examined. However, a statistically significant positive correlation was observed when non-infected individuals were considered separately ($F_{0,23}$=8.79, P=0.007; solid line in Fig. 2B) from individuals with immature ($F_{0,5}$=5.136, P=0.086) and mature ($F_{0,7}$=0.706, P=0.433) infections. Two-way

Table 2. F-statistics and associated *P*-values for effects of infection on body and tissue mass means

	Infection status				
Trait	NI	II	MI	*F*-ratio	*P*-value
Body mass (mg)	527.6±11.7	519.2±23.4	514.3±20.3	0.18	0.83
Thorax mass (mg)	296.7±7.3	298.5±14.6	285.3±12.6	0.35	0.71
Thorax/body mass	0.56±0.005	0.57±0.009	0.56±0.008	1.26	0.29
Basalar mass (mg)	16.7±0.5	16.3±1.0	17.7±0.9	0.68	0.51
Abdomen mass (mg)	96.1±2.9	94.0±5.7	94.0±5.0	0.10	0.91

Results of one-way ANOVA using infection status (NI, II, MI) as a predictor of mean±s.e.m. body mass, thorax mass (and their ratio), abdomen mass and basalar muscle mass (N=38; 24 NI, 6 II, 8 MI).

Journal of Experimental Biology (2019) 222, jeb188508. doi:10.1242/jeb.188508

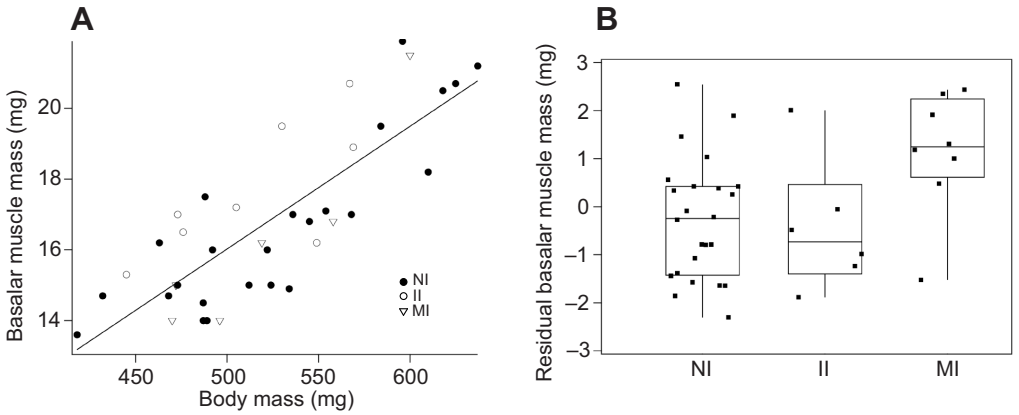

Fig. 1. Basalar muscle mass and infection status of *Libellula pulchella* dragonflies. (A) Fit of basalar muscle mass against body mass that generated the residuals plotted in B for *L. pulchella* with no infection (NI), with immature infection (II) and with mature infection (MI) with *Hoplorrhynchus* sp. gregarines. (B) Box plot (top horizontal bar in box represents third quartile, followed by median and first quartile; whiskers indicate data range) of residual basalar muscle mass, grouped by infection maturity: NI (N=24), II (N=6), MI (N=8). Jitter was applied to visualize individual data points.

ANOVA indicated that while body mass itself was not a significant predictor of power output ($F_{2,35}$=2.504, P=0.123), the interaction between body mass and infection status was highly significant ($F_{2,35}$=7.120, P=0.003, η^2=0.212), suggesting that infection affected the relationship between flight muscle power output and body mass.

Similarly, the relative abundance of *Tnt_Lp261* was positively correlated with body mass in non-infected individuals ($F_{0,23}$=7.10, P=0.0142; solid line in Fig. 2C), but not in individuals with immature ($F_{0,5}$=0.011, P=0.922) and mature ($F_{0,7}$=1.106, P=0.334) infections. Two-way ANOVA indicated that infection significantly reduced mean *Tnt_Lp261* relative abundance ($F_{2,35}$=4.18, P=0.024, η^2=0.177), while body mass, and the interaction between body mass and infection status were not significant predictors of *Tnt_Lp261* relative abundance ($F_{2,35}$=0.012, P=0.913, η^2=0.0003; $F_{2,35}$=2.074, P=0.142, η^2=0.088, respectively).

In contrast to *Tnt_Lp261*, there was no significant relationship between *Tnt_Lp258* (the most abundant *Tnt* splice variant) relative abundance and flight muscle power output for either non-infected, or individuals with immature and mature infections ($F_{0,23}$=0.670, P=0.422, $F_{0,5}$=0.333; P=0.594, $F_{0,7}$=5.757, P=0.053, respectively; Fig. 3A). Two-way ANOVA indicated that *Tnt_Lp258* relative abundance and its interaction with infection status, were non-significant predictors of flight muscle power output ($F_{2,35}$=3.324, P=0.078, $F_{2,35}$=0.243, P=0.786, respectively), while as before, infection status was a significant predictor of flight muscle power output ($F_{2,35}$=7.839, P=0.0017). Similarly, no significant correlation between body mass and *Tnt_Lp258* relative abundance was found for non-infected individuals ($F_{0,23}$=0.315, P=0.581) and individuals with immature or mature infections ($F_{0,5}$=0.029, P=0.873; $F_{0,7}$=0.076, P=0.792, respectively; Fig. 3B). Two-way ANOVA indicated that body mass, infection status or their interaction were not significant predictors of *Lp_Tnt258* relative abundance ($F_{2,35}$=0.031, P=0.862; $F_{2,35}$=0.216, P=0.807; $F_{2,35}$=0.095, P=0.909, respectively).

Infection effects on flight muscle power-frequency curves and comparison with tenerals

Male *L. pulchella* flight muscle power–cycle frequency curves, i.e. the performance behavior across the entire range of contractile frequencies (20–45 Hz) that we imposed on 54 (13 MI, 10 II, 31 NI) flight muscle preparations, were significantly affected by gregarine infection. Infection status ($F_{2,1401}$=65.20, P<0.0001), cycle frequency ($F_{2,1401}$=67.71, P<0.0001) and the infection status–cycle frequency interaction term ($F_{2,1401}$=2.04, P<0.0001) were all significant predictors of mean power output. The statistical

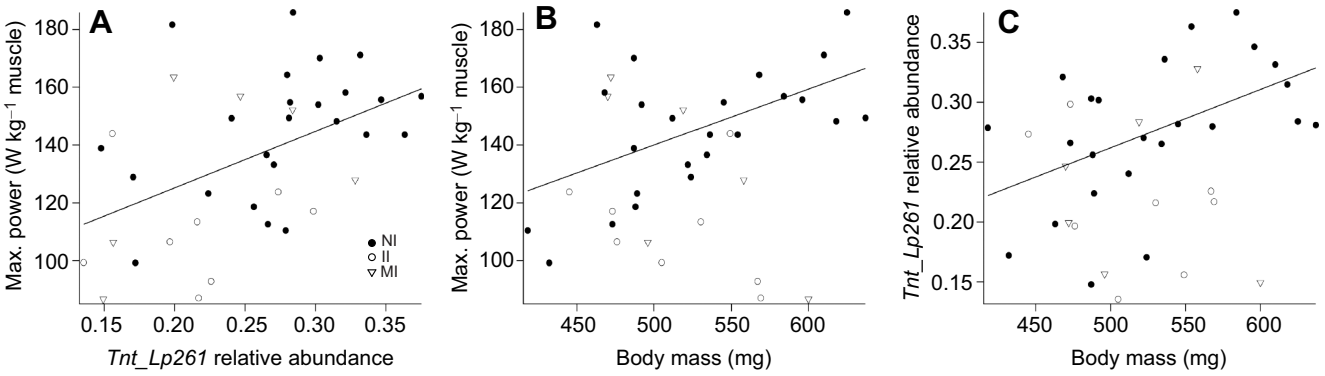

Fig. 2. Effects of gregarine infection on relationships between muscle power output, body mass and *Tnt* alternative splicing in *L. pulchella*. (A) Maximum mass-specific flight muscle power output as a function of *Tnt_Lp261* relative abundance (y=85.99+195.82x, R^2=0.233; N=38). (B) Maximum mass-specific flight muscle power output as a function of body mass, with a significant fit for NI individuals only (solid line; y=43.237+0.194x, R^2=0.286; N=24). (C) *Tnt_Lp261* relative abundance as a function of body mass, with a significant fit for NI individuals only (solid line; y=0.018+0.0005x, R^2=0.248; N=24). *Tnt_Lp261* relative abundance data were arcsine-transformed prior to fitting.

Journal of Experimental Biology (2019) 222, jeb188508. doi:10.1242/jeb.188508

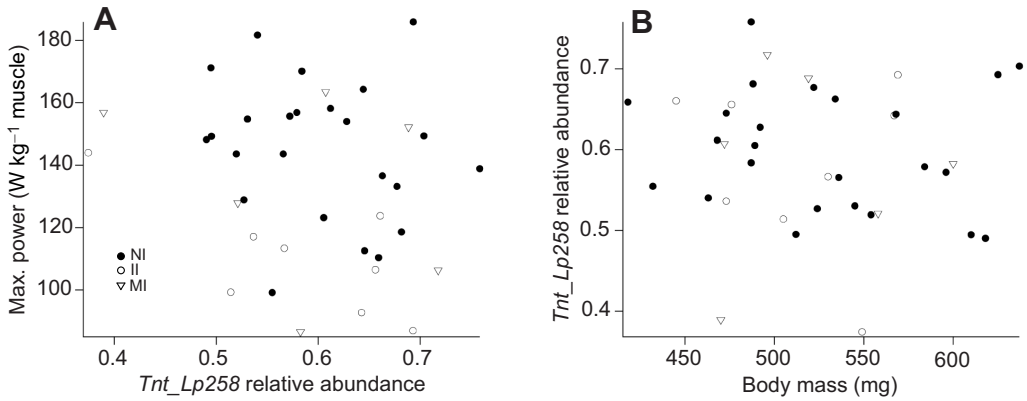

Fig. 3. *Tnt_Lp258* relative abundance does not correlate with flight muscle performance and body mass, and is not affected by infection. (A) Maximum mass-specific flight muscle power output as a function of *Tnt_Lp258* relative abundance. (B) *Tnt_Lp258* relative abundance as a function of body mass. *Tnt_Lp258* relative abundance data were arcsine-transformed prior to fitting.

significance of the interaction term suggested that the effect of infection was specific to certain cycle frequencies. Indeed, *post hoc* least-squares means contrast tests showed that muscle power output of NI individuals is significantly higher than that of MI individuals at higher cycle frequencies (38–45 Hz, $P \leq 0.00012$, $\alpha_{adj}=0.00064$; Fig. 4A). II individuals showed an intermediate power–cycle frequency relationship that was not statistically different from NI individuals, but was significantly different from MI individuals at 45 Hz ($P=0.00023$, $\alpha_{adj}=0.00064$; Fig. 4A).

The mean power–cycle frequency curve observed for MI individuals also resembled that of flight muscle preparations of teneral individuals. Addition of this fourth group (i.e. in addition to NI, II and MI) did not significantly change the outcome of the two-way, repeated-measures ANOVA as 'status' ($F_{3,1686}=55.04$, $P<0.0001$), cycle frequency ($F_{3,1686}=27.82$, $P<0.0001$) and the interaction term of cycle frequency and 'status' ($F_{3,1686}=3.68$, $P<0.0001$) were significant predictors of mean power output. *Post hoc* least-squares means contrast tests (of teneral versus NI, II, MI, for all cycle frequencies) showed that mean power output by tenerals was not significantly different from MI individuals at any cycle frequency, but was significantly lower than NI individuals at cycle frequencies of 36–45 Hz ($P \leq 0.00006$, $\alpha_{adj}=0.00032$; also see Fig. 4A) and lower than II individuals at cycle frequencies of 40–45 Hz ($P \leq 0.00023$, $\alpha_{adj}=0.00032$; also see Fig. 4A), respectively.

Thus, infection caused a significant reduction in the cycle frequency at which maximum performance was achieved (Fig. 4B). That is, a one-way ANOVA ($F_{3,63}=10.26$, $P<0.0001$, $\eta^2=0.332$) followed by *post hoc* LSmeans Tukey HSD test indicated that the mean cycle frequency at which maximum power output was achieved (i.e. optimal cycle frequency) was not different between NI and II individuals ($P=0.955$, Cohen's $d=0.174$). Mature infection caused a significant reduction in mean optimal cycle frequency ($P=0.0061$ and $P=0.0089$ for MI–NI and MI–II comparisons, respectively; Cohen's $d=1.232$ and 1.406, respectively), so that it was no different from mean optimal cycle frequency for teneral flight muscle preparations ($P=0.883$, Cohen's $d=0.321$).

DISCUSSION

This set of studies aimed to further our understanding of the effects of a non-lethal intestinal parasitic infection on flight performance in the dragonfly *L. pulchella* through a comparison of several skeletal muscle phenotypes known to be affected in obese vertebrates. We first demonstrated that infection is associated with an increase in mean relative basalar flight muscle mass (Fig. 2) in MI individuals.

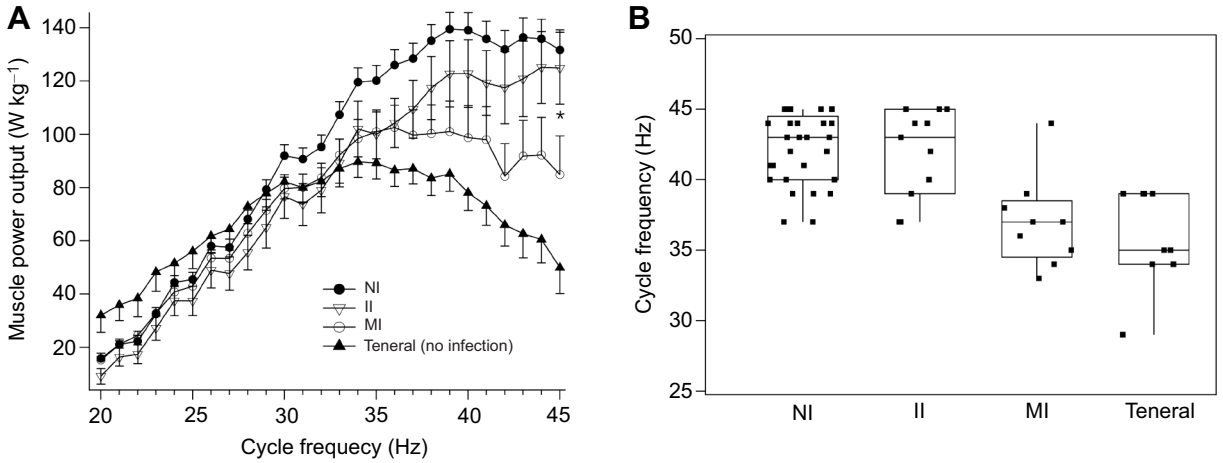

Fig. 4. Effect of infection and maturity level on power–cycle frequency curves. (A) Mean±s.e.m. flight muscle mass-specific power output as a function of cycle frequency (20–45 Hz) and status (i.e. NI, II, MI or teneral). For clarity, asterisks indicate statistically significant differences (at Bonferroni-adjusted $\alpha_{adj}=0.00064$) for comparisons of NI–MI and II–MI only (see Results for other comparisons). (B) Box plot (details as in Fig. 1B) of mean flight muscle cycle frequency at which maximum mass-specific power output was achieved, as a function of status. Jitter was applied to visualize individual data points.

Journal of Experimental Biology (2019) 222, jeb188508. doi:10.1242/jeb.188508

This was a somewhat unexpected finding as for both relative (i.e. normalized to total body mass) thoracic and abdominal mass there was no such effect of infection, suggesting that this effect is specific to the basalar muscle. While it is tempting to speculate that this result may reflect compensatory muscle growth to offset mass-specific performance loss during infection, this appears to not be the case and maximum absolute (i.e. non-normalized) power output is also significantly lower in infected individuals (data not shown). Muscle hypertrophy in insects is still poorly understood mechanistically, and typically described in the context of maturational or developmental muscle growth (Marden, 2000; Piccirillo et al., 2014). Even less well-studied are muscle mass and function dynamics in mature adult insects in response to natural aging and abiotic or biotic stressors such as infections. Our current findings in the *L. pulchella* system suggest that this may be a fruitful research avenue, and given that most insects suffer such stressors in nature, there may be many other invertebrate systems in which to examine the existence and relevance of locomotor muscle mass dynamics across their lifespan. Such studies could be relevant to biomedical research fields, because, for example, selective hypertrophy of load-bearing skeletal muscle occurs in obese vertebrates (Tomlinson et al., 2016) – even though skeletal muscle performance per unit mass is reduced (Bollinger, 2017; Lafortuna et al., 2005; Maffiuletti et al., 2007) – in highly similar fashion to results obtained in the current study.

Data presented in Fig. 2 indicate that infection impairs normal relationships between flight muscle performance, *Tnt* alternative splicing and body mass. Interestingly, this impairment is similar to that observed in rats in whom obesity develops as a result of genetically induced hyperphagy (i.e. Zucker rats; Schilder et al., 2011). In healthy rats (Marden et al., 2008; Schilder and Raynor, 2017), *Tnt* alternative splicing is adjusted in a quantitative fashion in response to body weight changes due to natural growth or experimental body weight manipulations. Our current study suggests that similar, body weight-dependent adjustments in *Tnt* alternative splicing occur in *L. pulchella* flight muscle, as in non-infected individuals there was a statistically significant, positive correlation between body mass and the relative abundance of *Tnt_Lp261* (Fig. 2C), one of two highly abundant *Tnt* splice variants in this tissue (see Table 1). In addition to signals reflecting quantitative variation in body weight, *Tnt* alternative splicing in mammals and insects is sensitive to dietary quantity and quality (Marden et al., 2008; Black et al., 2017; Portman et al., 2015). Moreover, in non-infected *L. pulchella* males, flight muscle power output is correlated with total body fat content, but this correlation is absent in infected males (Marden and Cobb, 2004).

Combined, these observations from different vertebrate and insect systems suggest that in healthy organisms, muscle performance can be adjusted by an unknown mechanism that integrates the input of sensors receiving information about body weight and energetic status. It appears that in insects and vertebrates alike, *Tnt* alternative splicing is a useful molecular trait to study this mechanism, although it likely represents a much larger suite of sarcomere and non-sarcomere genes whose expression is controlled by this mechanism (Black et al., 2017).

Mature gregarine infections also caused a change in the shape of *L. pulchella* flight muscle power–cycle frequency curves (Fig. 4A), as mean optimal cycle frequency in MI individuals was significantly reduced compared with mean values in NI and II (Fig. 4B). This finding is supported by the observed effects of infection on flight muscle *Tnt_Lp261* relative abundance (Fig. 2), which are expected to lower flight muscle calcium sensitivity, and mass-specific performance at higher cycle frequencies (Marden et al., 1998; Marden et al., 2001). Interestingly, this left-shifted power-cycle frequency curve of MI individuals was not significantly different from that produced by flight muscles of teneral *L. pulchella* males, and is also similar to the results recently obtained for obese zebrafish (Seebacher et al., 2017). Seebacher et al. (2017) suggested that this loss of performance at higher contractile frequencies may be explained by the overall reduction in both slow and fast MyHC content (i.e. reduced overall myofibrillar density) that they observed in obese zebrafish individuals. That study also noted that this defect may be due to impairment of signaling pathways that mediate expression of multiple muscle sarcomere proteins (Bassel-Duby and Olson, 2006; Watts et al., 2013, in: Seebacher et al., 2017). Our results in Fig. 2 showing a disruption of normal relationships between *Tnt* alternative splicing, body mass and flight muscle power output appear to be in agreement with this notion, even if they do not address MyHC protein expression.

As discussed in the Introduction, it remains unclear whether functionally distinct MyHC protein isoforms are expressed in insect flight muscle as in mammalian skeletal muscles, but, related to the

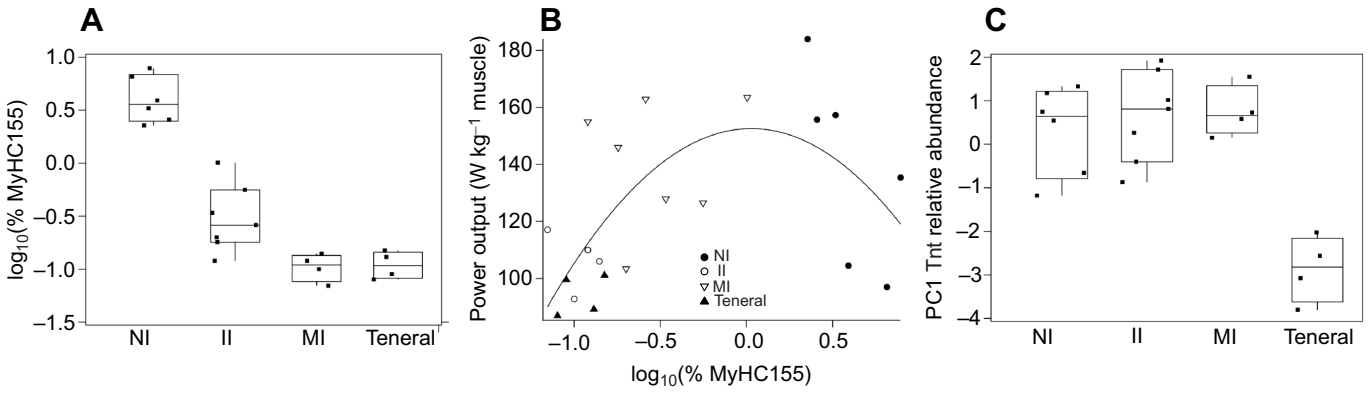

Fig. 5. Comparison of teneral and mature *L. pulchella* flight muscle sarcomere protein expression using 2D PAGE. Teneral protein expression data was added to a previously published dataset for mature *L. pulchella* males (Schilder and Marden, 2007) and the complete dataset was re-analyzed. (A) $\log_{10}$-transformed quantities (% of total protein on 2D gels; see Materials and Methods) of a 155 kDa, proteolytic degradation product of MyHC (MyHC155) as a function of infection status. (B) A significant second-order polynomial fit (y=163.2+35.9x–59.2x^2; F-ratio=7.114, P=0.0053) describing the relationship between maximum mass-specific flight muscle power output as a function of $\log_{10}$(%MyHC155) for all data (N=21). (C) Box plot (details as in Fig. 1B) showing Tnt protein isoform expression (summarized as the first principal component; see Materials and Methods) as a function of infection status.

zebrafish findings above, we did previously demonstrate that gregarine gut infections are associated with a significant reduction of *L. pulchella* flight muscle quantities of a (putative) MyHC proteolytic degradation product (MyHC155; Schilder and Marden, 2007). Using the same methodology as in that paper (see Materials and Methods), we here show that the quantity of teneral flight muscle MyHC155 on 2D PAGE gels (Fig. 5A) and its relationship with flight muscle power output (Fig. 5B) are similar to that of flight muscles of MI individuals (P=0.999) but significantly different from NI and II individuals (P<0.0001, P=0.0372, respectively; Fig. 5A,B).

How might this reduction in flight muscle quantities of MyHC155 relate to flight muscle performance? Interestingly, MI individuals have significantly increased flight muscle mass (Fig. 1) but with lower maximum mass-specific power output (Schilder and Marden, 2006; Fig. 4A). It is therefore possible that relatively low levels of MyHC155 (i.e. MyHC degradation) reflect relatively low overall flight muscle MyHC protein production in MI individuals, which may contribute to the reduction of muscle mass-specific performance at higher contractile frequencies, as was suggested for obese zebrafish muscle (see above; Seebacher et al., 2017). Alternatively, MyHC degradation could be lower in MI individuals, and similar to that in teneral flight muscle, because of infection-induced reduction of flight behavior intensity (Marden and Cobb, 2004; Schilder and Marden, 2006) and, associated with this, reduced intensity of overall sarcomere protein use (for further discussion, see Schilder and Marden, 2007). Unfortunately we do not have data on infection effects on myofibrillar protein density (i.e. sarcomere protein content per unit muscle mass), so this has to remain a speculative set of ideas.

While in this study we did not quantify *Tnt* mRNA splice variant abundance for teneral flight muscles, the same 2D PAGE analyses indicated that overall teneral flight muscles Tnt protein expression (i.e. PC1 Tnt relative abundance) is significantly different from mature adults, irrespective of their infection status (P<0.0001 for all comparisons; Fig. 5C). Therefore, teneral flight muscle appears to be similar to that of MI individuals with respect to MyHC degradation dynamics, but different at the level of Tnt protein expression, suggesting that different combinations of sarcomere traits may yield similar physiological phenotypes (e.g. power–cycle frequency curves) in these two groups.

Regardless of the exact molecular traits involved, the similarity of power–cycle frequency curves between MI and teneral individuals does raise the interesting question as to whether the parasite is directly manipulating the dragonfly host physiology and behavior for its benefit or if infected mature male *L. pulchella* may be adopting a low-intensity more energy efficient behavioral strategy to cope with metabolic impairments caused by infection. Gregarine parasites potentially use excretory chemicals to manipulate their dragonfly host (Schilder and Marden, 2006), but currently available data on these chemical interactions do not yet allow us to distinguish between these two scenarios definitively.

While it is evident that the non-lethal gregarine infection has significant effects on multiple aspects of *L. pulchella* flight physiology, we remain somewhat cautious with our comparisons to mammalian obesity, as currently available data limit us to identification of associations of these effects with infection, rather than exact mechanisms through which these effects are accomplished. Here, we have demonstrated that relationships between *Tnt* alternative splicing, body mass and flight muscle contractile performance are affected in *L. pulchella* males in similar ways to those described for obese mammals and fish. However, as appears to be the case with these vertebrate systems, our understanding of molecular mechanisms that lead to these impairments is still incomplete. Nonetheless, what should be evident from this study is that metabolic disease syndromes with a high degree of similarity to mammalian obesity and diabetes exist in nature, and that detailed study of additional natural systems may provide pertinent information regarding environmental factors that can contribute (in parallel, or interactively with effects of diet and exercise) to the development of such syndromes. As mentioned earlier, it is possible that flying insect systems such as dragonflies are particularly vulnerable to homeostatic disturbance caused by such environmental factors (e.g. parasitic infections) due to their ‘high-octane’ lifestyle, but given that gregarine infections are common in arthropods (Smith and Clopton, 2003), this possibility can be readily explored through the study of other species.

Acknowledgements
The authors would like to thank two anonymous reviewers, whose comments greatly improved the manuscript.

Competing Interests
The authors declare no competing or financial interests.

Author contributions
Conceptualization: R.J.S.; Methodology: R.J.S.; Formal analysis: R.J.S.; Investigation: R.J.S., H.S.; Data curation: R.J.S., H.S.; Writing - original draft: R.J.S.; Writing - review & editing: R.J.S., H.S.; Visualization: R.J.S.; Supervision: R.J.S.; Project administration: R.J.S.; Funding acquisition: R.J.S.

Funding
This work was supported by a grant from the National Science Foundation (NSF-IOS 1457237) to R.J.S.

References
Altizer, S., Hobson, K. A., Davis, A. K., De Roode, J. C. and Wassenaar, L. I. (2015). Do healthy monarchs migrate farther? tracking natal origins of parasitized vs. uninfected monarch butterflies overwintering in Mexico. *PLoS ONE* **10**, e0141371.

Arrese, E. L. and Soulages, J. L. (2010). Insect fat body: energy, metabolism, and regulation. *Annu. Rev. Entomol.* **55**, 207-225.

Ayme-Southgate, A., Feldman, S. and Fulmer, D. (2015). Myofilament proteins in the synchronous flight muscles of Manduca sexta show both similarities and differences to *Drosophila melanogaster*. *Insect Biochem. Mol. Biol.* **62**, 174-182.

Bassel-Duby, R. and Olson, E. N. (2006). Signaling pathways in skeletal muscle remodeling. *Annu. Rev. Biochem.* **75**, 19-37.

Beutler, B. (2004). Innate immunity: an overview. *Mol. Immunol.* **40**, 845-859.

Birse, R. T. R., Choi, J. J., Reardon, K. K., Rodriguez, J. J., Graham, S. S., Diop, S. S., Ocorr, K. K., Bodmer, R. R. and Oldham, S. S. (2010). High-fat-diet-induced obesity and heart dysfunction are regulated by the TOR pathway in Drosophila. *Cell Metab.* **12**, 533-544.

Black, A. J., Ravi, S., Jefferson, L. S., Kimball, S. R. and Schilder, R. J. (2017). Dietary fat quantity and type induce transcriptome-wide effects on alternative splicing of pre-mRNA in rat skeletal muscle. *J. Nutr.* **147**, 1648-1657.

Bollinger, L. M. (2017). Potential contributions of skeletal muscle contractile dysfunction to altered biomechanics in obesity. *Gait Posture* **56**, 100-107.

Briggs, M. M. and Schachat, F. (1996). Physiologically regulated alternative splicing patterns of fast troponin T RNA are conserved in mammals. *Am. J. Physiol.* **270**, C298-C305.

Candy, D. J. and Kilby, B. A. (ed.) (1975). *Insect Biochemistry and Function*. Chapman and Hall.

Coble, J., Schilder, R. J., Berg, A., Drummond, M. J., Rasmussen, B. B. and Kimball, S. R. (2015). Influence of ageing and essential amino acids on quantitative patterns of troponin T alternative splicing in human skeletal muscle. *Appl. Physiol. Nutr. Metab. Physiol. Appliquée Nutr. Métabolisme* **40**, 788-796.

Denies, M. S., Johnson, J., Maliphol, A. B., Bruno, M., Kim, A., Rizvi, A., Rustici, K. and Medler, S. (2014). Diet-induced obesity alters skeletal muscle fiber types of male but not female mice. *Physiol. Rep.* **2**, e00204.

Dhurandhar, N. V. (2011). A framework for identification of infections that contribute to human obesity. *Lancet Infect. Dis.* **11**, 963-969.

Dosselli, R., Grassl, J., Carson, A., Simmons, L. W. and Baer, B. (2016). Flight behaviour of honey bee (*Apis mellifera*) workers is altered by initial infections of the fungal parasite *Nosema apis*. *Sci. Rep.* **6**, 36649.

Dudley, R. (2002). Mechanisms and implications of animal flight maneuverability. *Integr. Comp. Biol.* **42**, 135-140.
Dussaubat, C., Maisonnasse, A., Crauser, D., Beslay, D., Costagliola, G., Soubeyrand, S., Kretzchmar, A. and Le Conte, Y. (2013). Flight behavior and pheromone changes associated to *Nosema ceranae* infection of honey bee workers (*Apis mellifera*) in field conditions. *J. Invertebr. Pathol.* **113**, 42-51.
Fenton, P. F. and Dowling, M. T. (1953). Studies on obesity. I. Nutritional obesity in mice. *J. Nutr.* **49**, 319-331.
Fitzhugh, G. and Marden, J. (1997). Maturational changes in troponin T expression, Ca2+-sensitivity and twitch contraction kinetics in dragonfly flight muscle. *J. Exp. Biol.* **200**, 1473-1482.
Gilmour,, D. (1965). *The Metabolism of Insects*. Oliver and Boyd Ltd.
Goodpaster, B. H. and Wolf, D. (2004). Skeletal muscle lipid accumulation in obesity, insulin resistance, and type 2 diabetes. *Pediatr. Diabetes* **5**, 219-226.
Greaser, M. L., Moss, R. L. and Reiser, P. J. (1988). Variations in contractile properties of rabbit single muscle fibres in relation to troponin T isoforms and myosin light chains. *J. Physiol.* **406**, 85-98.
Harrison, J. F., Camazine, S., Marden, J. H., Kirkton, S. D., Rozo, A. and Yang, X. (2001). Mite not make it home: tracheal mites reduce the safety margin for oxygen delivery of flying honeybees. *J. Exp. Biol.* **204**, 805-814.
Hoffmann, J. A., Kafatos, F. C., Janeway, C. A. and Ezekowitz, R. a. B. (1999). Phylogenetic perspectives in innate immunity. *Science* **284**, 1313-1318.
Hooper, S. L. and Thuma, J. B. (2005). Invertebrate muscles: muscle specific genes and proteins. *Physiol. Rev.* **85**, 1001-1060.
Ingle, D. J. (1949). A simple means of producing obesity in the rat. *Proc. Soc. Exp. Biol. Med. Soc. Exp. Biol. Med. N. Y. N* **72**, 604.
Kelley, D. E. and Goodpaster, B. H. (2001). Skeletal muscle triglyceride: an aspect of regional adiposity and insulin resistance. *Diabe. Care* **24**, 933-941.
Khovidhunkit, W., Kim, M.-S., Memon, R. A., Shigenaga, J. K., Moser, A. H., Feingold, K. R. and Grunfeld, C. (2004). Thematic review series: the pathogenesis of atherosclerosis. Effects of infection and inflammation on lipid and lipoprotein metabolism mechanisms and consequences to the host. *J. Lipid Res.* **45**, 1169-1196.
Kimbrell, D. A. and Beutler, B. (2001). The evolution and genetics of innate immunity. *Nat. Rev. Genet.* **2**, 256-267.
Klimentidis, Y. C., Beasley, T. M., Lin, H.-Y., Murati, G., Glass, G. E., Guyton, M., Newton, W., Jorgensen, M., Heymsfield, S. B. and Kemnitz, J. (2011). Canaries in the coal mine: a cross-species analysis of the plurality of obesity epidemics. *Proc. R. Soc. B Biol. Sci.* **278**, 1626-1632.
Lafortuna, C. L., Maffiuletti, N. A., Agosti, F. and Sartorio, A. (2005). Gender variations of body composition, muscle strength and power output in morbid obesity. *Int. J. Obes.* **29**, 833-841.
Li, J., Lu, Z., He, J., Chen, Q., Wang, X., Kang, L. and Li, X. –. (2016). Alternative exon-encoding regions of *Locusta migratoria* muscle myosin modulate the pH dependence of ATPase activity. *Insect Mol. Biol.* **25**, 689-700.
Maffiuletti, N. A., Jubeau, M., Munzinger, U., Bizzini, M., Agosti, F., Col, A. D., Lafortuna, C. L. and Sartorio, A. (2007). Differences in quadriceps muscle strength and fatigue between lean and obese subjects. *Eur. J. Appl. Physiol.* **101**, 51-59.
Marden, J. H. (2000). Variability in the Size, composition, and function of insect flight muscles. *Annu. Rev. Physiol.* **62**, 157-178.
Marden, J. H. and Cobb, J. R. (2004). Territorial and mating success of dragonflies that vary in muscle power output and presence of gregarine gut parasites. *Anim. Behav.* **68**, 857-865.
Marden, J. H., Fitzhugh, G. H. and Wolf, M. R. (1998). From molecules to mating success: integrative biology of muscle maturation in a dragonfly. *Am. Zool.* **38**, 528-544.
Marden, J. H., Fitzhugh, G. H., Wolf, M. R., Arnold, K. D. and Rowan, B. (1999). Alternative splicing, muscle calcium sensitivity, and the modulation of dragonfly flight performance. *Proc. Natl. Acad. Sci. USA* **96**, 15304-15309.
Marden, J. H., Fitzhugh, G. H., Girgenrath, M., Wolf, M. R. and Girgenrath, S. (2001). Alternative splicing, muscle contraction and intraspecific variation: associations between troponin T transcripts, Ca2+ sensitivity and the force and power output of dragonfly flight muscles during oscillatory contraction. *J. Exp. Biol.* **204**, 3457-3470.
Marden, J. H., Fescemyer, H. W., Saastamoinen, M., Macfarland, S. P., Vera, J. C., Frilander, M. J. and Hanski, I. (2008). Weight and nutrition affect pre-mRNA splicing of a muscle gene associated with performance, energetics and life history. *J. Exp. Biol.* **211**, 3653-3660.
Martinelli, C. and Reichhart, J.-M. (2005). Evolution and integration of innate immune systems from fruit flies to man: lessons and questions. *J. Endotoxin Res.* **11**, 243-248.
Maughan, D. and Swank, D. (2013). *Insect Flight Muscle Chemomechanics*. Landes Bioscience.
May, M. L. (1991). Dragonfly flight: power requirements at high speed and acceleration. *J. Exp. Biol.* **158**, 325-342.
McAllister, E. J., Dhurandhar, N. V., Keith, S. W., Aronne, L. J., Barger, J., Baskin, M., Benca, R. M., Biggio, J., Boggiano, M. M., Eisenmann, J. C. et al. (2009). Ten putative contributors to the obesity epidemic. *Crit. Rev. Food Sci. Nutr.* **49**, 868-913.
Mead, A. F., Osinalde, N., Ørtenblad, N., Nielsen, J., Brewer, J., Vellema, M., Adam, I., Scharff, C., Song, Y., Frandsen, U. et al. (2017). Fundamental constraints in synchronous muscle limit superfast motor control in vertebrates. *eLife* **6**, e29425.
Moss, R. L., Diffee, G. M. Greaser, M. L. (1995). Contractile properties of skeletal muscle fibers in relation to myofibrillar protein isoforms. *Rev. Physiol. Biochem. Pharmacol.* **126**, 1-63.
Nassar, R., Malouf, N. N., Kelly, M. B., Oakeley, A. E. and Anderson, P. A. (1991). Force-pCa relation and troponin T isoforms of rabbit myocardium. *Circ. Res.* **69**, 1470-1475.
Newman, C. M., Anderson, T. K. and Goldberg, T. L. (2016). Decreased flight activity in Culex Pipiens (Diptera: Culicidae) naturally infected with Culex Flavivirus. *J. Med. Entomol.* **53**, 233-236.
Palmer, W. J. and Jiggins, F. M. (2015). Comparative genomics reveals the origins and diversity of arthropod immune systems. *Mol. Biol. Evol.* **32**, 2111-2129.
Pasarica, M. and Dhurandhar, N. V. (2007). Infectobesity: obesity of infectious origin. *Adv. Food Nutr. Res.* **52**, 61-102.
Perry, S. (1998). Troponin T: Genetics, properties and function. *J. Muscle Res. Cell Motil.* **19**, 575-602.
Perseghin, G. (2005). Muscle lipid metabolism in the metabolic syndrome. *Curr. Opin. Lipidol.* **16**, 416-420.
Piccirillo, R., Demontis, F., Perrimon, N. and Goldberg, A. L. (2014). Mechanisms of muscle growth and atrophy in mammals and drosophila. *Dev. Dyn. Off. Publ. Am. Assoc. Anat.* **243**, 201-215.
Portman, S. L., Kariyat, R. R., Johnston, M. A., Stephenson, A. G. and Marden, J. H. (2015). Cascading effects of host plant inbreeding on the larval growth, muscle molecular composition, and flight capacity of an adult herbivorous insect. *Funct. Ecol.* **29**, 328-337.
Reiser, P. J., Westfall, M. and Solaro, R. J. (1990). Developmental transition in myocardial troponin T (TnT) isoforms correlates with a change in calcium sensitivity. *Biophys. J.* **57**, 549A.
Ritov, V. B., Menshikova, E. V., He, J., Ferrell, R. E., Goodpaster, B. H. and Kelley, D. E. (2005). Deficiency of subsarcolemmal mitochondria in obesity and Type 2 diabetes. *Diabetes* **54**, 8-14.
Rowland, M. and Boersma, E. (1988). Changes in the spontaneous flight activity of the mosquito Anopheles stephensi by parasitization with the rodent malaria *Plasmodium yoelii*. *Parasitology* **97** , 221-227.
Rüppell, G. (1989). Kinematic analysis of symmetrical flight manoeuvres of odonata. *J. Exp. Biol.* **144**, 13-42.
Sacktor, B. (1975). Biochemistry of insect flight. 1. Utilization of fuels by muscle. In *Insect Biochemistry and Function* (ed. D. J. Candy and B. A. Kilby), pp. 3-88. Chapman and Hall.
Schachat, F. H., Diamond, M. S. and Brandt, P. W. (1987). Effect of different troponin T-tropomyosin combinations on thin filament activation. *J. Mol. Biol.* **198**, 551-554.
Schilder, R. J. and Marden, J. H. (2004). A hierarchical analysis of the scaling of force and power production by dragonfly flight motors. *J. Exp. Biol.* **207**, 767-776.
Schilder, R. J. and Marden, J. H. (2006). Metabolic syndrome and obesity in an insect. *Proc. Natl. Acad. Sci.* **103**, 18805-18809.
Schilder, R. J. and Marden, J. H. (2007). Parasites, proteomics and performance: effects of gregarine gut parasites on dragonfly flight muscle composition and function. *J. Exp. Biol.* **210**, 4298-4306.
Schilder, R. J. and Raynor, M. (2017). Molecular plasticity and functional enhancements of leg muscles in response to hypergravity in the fruit fly *Drosophila melanogaster*. *J. Exp. Biol.* **220**, 3508-3518.
Schilder, R. J., Kimball, S. R., Marden, J. H. and Jefferson, L. S. (2011). Body weight-dependent troponin T alternative splicing is evolutionarily conserved from insects to mammals and is partially impaired in skeletal muscle of obese rats. *J. Exp. Biol.* **214**, 1523-1532.
Schlegel, A. and Stainier, D. Y. R. (2007). Lessons from “lower” organisms: what worms, flies, and zebrafish can teach us about human energy metabolism. *PLoS Genet.* **3**, e199.
Schönke, M., Björnholm, M., Chibalin, A. V., Zierath, J. R. and Deshmukh, A. S. (2018). Proteomics analysis of skeletal muscle from leptin-deficient ob/ob mice reveals adaptive remodeling of metabolic characteristics and fiber type composition. *Proteomics* **18**, 1700375.
Seebacher, F., Tallis, J., McShea, K. and James, R. S. (2017). Obesity-induced decreases in muscle performance are not reversed by weight loss. *Int. J. Obes.* **41**, 1271-1278.
Simmons, P. (1977). The neuronal control of dragonfly flight. II. Physiology. *J. Exp. Biol.* **71**, 141-155.
Smith, A. J. and Clopton, R. E. (2003). Efficacy of oral metronidazole and potassium sorbate against two gregarine parasites, *Protomagalhaensia granulosae* and *Gregarina cubensis* (apicomplexa: eugregarinida), infecting the death’s head cockroach, *Blaberus discoidalis*. *Comp. Parasitol.* **70**, 196-199.
Solaro, R. J. and Rarick, H. M. (1998). Troponin and tropomyosin: proteins that switch on and tune in the activity of cardiac myofilaments. *Circ. Res.* **83**, 471-480.
Sonnenburg, J. L., Chen, C. T. L. and Gordon, J. I. (2006). Genomic and metabolic studies of the impact of probiotics on a model gut symbiont and host. *PLoS Biol.* **4**, e413.

Steinberg, G. R. (2007). Inflammation in obesity is a common link between defects in fatty acid metabolism and insulin resistance. *Cell Cycle* **6**, 888-894.
Sweeney, H. L., Bowman, B. F. and Stull, J. T. (1993). Myosin light chain phosphorylation in vertebrate striated muscle: regulation and function. *Am. J. Physiol.* **264**, C1085-C1095.
Tallis, J., Hill, C., James, R. S., Cox, V. M. and Seebacher, F. (2017). The effect of obesity on the contractile performance of isolated mouse soleus, EDL, and diaphragm muscles. *J. Appl. Physiol.* **122**, 170-181.
Tallis, J., James, R. S. and Seebacher, F. (2018). The effects of obesity on skeletal muscle contractile function. *J. Exp. Biol.* **221**, jeb163840.
Tanner, C. J., Barakat, H. A., Dohm, G. L., Pories, W. J., MacDonald, K. G., Cunningham, P. R. G., Swanson, M. S. and Houmard, J. A. (2002). Muscle fiber type is associated with obesity and weight loss. *Am. J. Physiol. Endocrinol. Metab.* **282**, E1191-E1196.
Tomlinson, D. J., Erskine, R. M., Morse, C. I., Winwood, K. and Onambélé-Pearson, G. (2016). The impact of obesity on skeletal muscle strength and structure through adolescence to old age. *Biogerontology* **17**, 467-483.
Turnbaugh, P. J., Ley, R. E., Mahowald, M. A., Magrini, V., Mardis, E. R. and Gordon, J. I. (2006). An obesity-associated gut microbiome with increased capacity for energy harvest. *Nature* **444**, 1027-1031.
Watts, R., McAinch, A. J., Dixon, J. B., O'Brien, P. E. and Cameron-Smith, D. (2013). Increased Smad signaling and reduced MRF expression in skeletal muscle from obese subjects. *Obes. Silver Spring Md* **21**, 525-528.
Wolf, S., McMahon, D. P., Lim, K. S., Pull, C. D., Clark, S. J., Paxton, R. J. and Osborne, J. L. (2014). So near and yet so far: harmonic radar reveals reduced homing ability of Nosema infected honeybees. *PLoS ONE* **9**, e103989.
Yee, W. L. and Anderson, J. R. (1995). Free flight of *Lambornella clarki*-infected, blood-fed, and gravid *Aedes sierrensis* (Diptera: Culicidae). *J. Med. Entomol.* **32**, 407-412.
Ziegler, C., Ader, G. and Beinbrech, G. (1994). Evidence for two myosin types in indirect insect flight muscles. *Comp. Biochem. Physiol. Part B Comp. Biochem.* **107**, 91-98.